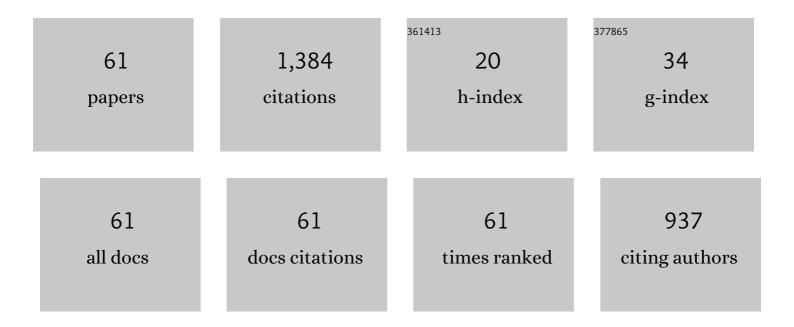
Ehsan Shakerzadeh

List of Publications by Year in descending order

Source: https://exaly.com/author-pdf/7879328/publications.pdf Version: 2024-02-01



#	Article	IF	CITATIONS
1	Shannon entropy as a new measure of aromaticity, Shannon aromaticity. Physical Chemistry Chemical Physics, 2010, 12, 4742.	2.8	153
2	Theoretical assessment of the electro-optical features of the group III nitrides (B12N12, Al12N12 and) Tj ETQ metals (Li, Na and K). Applied Surface Science, 2016, 363, 197-208.	q0 0 0 rgBT / 6.1	Overlock 10 T 83
3	Formaldehyde adsorption on pristine, Al-doped and mono-vacancy defected boron nitride nanosheets: A first principles study. Computational Materials Science, 2012, 56, 122-130.	3.0	76
4	M@B40 (M = Li, Na, K) serving as a potential promising novel NLO nanomaterial. Chemical Physics Letters, 2016, 654, 76-80.	2.6	71
5	A New Scale of Electronegativity Based on Electrophilicity Index. Journal of Physical Chemistry A, 2008, 112, 3486-3491.	2.5	58
6	A comparative theoretical study on the structural, electronic and nonlinear optical features of B12N12 and Al12N12 nanoclusters with the groups III, IV and V dopants. Superlattices and Microstructures, 2014, 76, 264-276.	3.1	57
7	Theoretical assessment of phosgene adsorption behavior onto pristine, Al- and Ga-doped B12N12 and B16N16 nanoclusters. Computational Materials Science, 2016, 118, 155-171.	3.0	45
8	A comparative theoretical study of CO2 sensing using inorganic AlN, BN and SiC single walled nanotubes. Sensors and Actuators B: Chemical, 2013, 185, 512-522.	7.8	42
9	A first principles study of pristine and Al-doped boron nitride nanotubes interacting with platinum-based anticancer drugs. Physica E: Low-Dimensional Systems and Nanostructures, 2014, 57, 47-55.	2.7	39
10	The Al, Ga and Sc dopants effect on the adsorption performance of B12N12 nanocluster toward pnictogen hydrides. Chemical Physics, 2019, 526, 110424.	1.9	37
11	A quantum chemical study on the remarkable nonlinear optical and electronic characteristics of boron nitride nanoclusters by complexation via lithium atom. Journal of Molecular Liquids, 2016, 221, 443-451.	4.9	32
12	Ngn (Ng= Ne, Ar, Kr, Xe, and Rn; n=1, 2) encapsulated porphyrin-like porous C24N24 fullerene: A quantum chemical study. Journal of Molecular Graphics and Modelling, 2021, 108, 107986.	2.4	30
13	Quantum chemical assessment of the adsorption behavior of fluorouracil as an anticancer drug on the B 36 nanosheet. Journal of Molecular Liquids, 2017, 240, 682-693.	4.9	29
14	Theoretical approach into potential possibility of efficient NO2 detection via B40 and Li@B40 fullerenes. Chemical Physics Letters, 2018, 691, 360-365.	2.6	27
15	Magnesiation of bare and halides encapsulated B40 fullerenes for their potential application as promising anode materials for Mg-ion batteries. Applied Surface Science, 2021, 538, 148060.	6.1	27
16	Computational mechanistic insights into CO oxidation reaction over Fe decorated C24N24 fullerene. Inorganic Chemistry Communication, 2019, 106, 190-196.	3.9	26
17	Nonlinear Optical (NLO) Response of Pristine and Functionalized Dodecadehydrotribenzo[18]annulene ([18]DBA): A Theoretical Study. Bulletin of the Chemical Society of Japan, 2016, 89, 692-699.	3.2	25
18	A DFT study on the formaldehyde (H 2 CO and (H 2 CO) 2) monitoring using pristine B 12 N 12 nanocluster. Physica E: Low-Dimensional Systems and Nanostructures, 2016, 78, 1-9.	2.7	25

#	Article	IF	CITATIONS
19	Efficient carriers for anticancer 5-fluorouracil drug based on the bare and Mâ^'encapsulated (M = Na) Tj ETQo	1_10.784 4.9	+314 rgBT ∣O
20	Enhanced electronic and nonlinear optical responses of C ₂₄ N ₂₄ cavernous nitride fullerene by decoration with first row transition metals; A computational investigation. Applied Organometallic Chemistry, 2020, 34, e5694.	3.5	23
21	Bond dissociation energies from a new electronegativity scale. Journal of Molecular Structure, 2009, 920, 110-113.	3.6	22
22	How Does Lithiation Affect Electro-Optical Features of Corannulene (C20H10) and Quadrannulene (C16H8) Buckybowls?. Journal of Electronic Materials, 2018, 47, 2348-2358.	2.2	22
23	Can C24N24 cavernous nitride fullerene be a potential anode material for Li-, Na-, K-, Mg-, Ca-ion batteries?. Chemical Physics Letters, 2021, 764, 138241.	2.6	22
24	Pristine and alkali and alkaline earth metals encapsulated B ₃₆ N ₃₆ nanoclusters as prospective delivery agents and detectors for 5â€fluorouracil anticancer drug. Applied Organometallic Chemistry, 2022, 36, .	3.5	22
25	Acetylsalicylic acid interaction with Boron nitride nanostructures – A density functional analysis. Journal of Molecular Liquids, 2022, 355, 118980.	4.9	21
26	A DFT study on the potential application of Si@C24N24 porous fullerene as an innovative and highly active catalyst for NO reduction. Chemical Physics Letters, 2019, 724, 80-85.	2.6	19
27	Synthesis, structural characterization, and density functional theory calculations of the two new Zn (II) complexes as antibacterial and anticancer agents with a neutral flexible tetradentate pyrazoleâ€based ligand. Applied Organometallic Chemistry, 2021, 35, e6173.	3.5	18
28	Electro-optical properties of bowl-like B36 cluster doped with the first row transition metals: A DFT insight. Physica E: Low-Dimensional Systems and Nanostructures, 2019, 114, 113599.	2.7	17
29	Li@B40 and Na@B40 fullerenes serving as efficient carriers for anticancer nedaplatin drug: A quantum chemical study. Computational and Theoretical Chemistry, 2021, 1202, 113339.	2.5	17
30	Fe-decorated all-boron B40 fullerene serving as a potential promising active catalyst for CO oxidation: A DFT mechanistic approach. Polyhedron, 2020, 188, 114699.	2.2	16
31	A comparative DFT study on prospective application of C24, Si12C12, B12N12, B12P12, Al12N12, and Al12P12 nanoclusters as suitable anode materials for magnesium-ion batteries (MIBs). Physica E: Low-Dimensional Systems and Nanostructures, 2022, 140, 115161.	2.7	16
32	A Theoretical Study on the Influence of Carbon and Silicon Doping on the Structural and Electronic Properties of (BeO)12 Nanocluster. Journal of Inorganic and Organometallic Polymers and Materials, 2014, 24, 694-705.	3.7	15
33	Electronic and nonlinear optical features of first row transition metals-decorated all-boron B40 fullerene: A promising route to remarkable electro-optical response. Inorganic Chemistry Communication, 2020, 112, 107692.	3.9	15
34	Li n @B36 (nÂ=Â1, 2) Nanosheet with Remarkable Electro-Optical Properties: A DFT Study. Journal of Electronic Materials, 2017, 46, 4420-4425.	2.2	14
35	The scandium doped boron cluster B ₂₇ Sc ₂ ⁺ : a fruit can-like structure. Physical Chemistry Chemical Physics, 2019, 21, 8933-8939.	2.8	14
36	Selective detection of toxic cyanogen gas in the presence of O 2 , and H 2 O molecules using a AlN nanocluster. Physics Letters, Section A: General, Atomic and Solid State Physics, 2016, 380, 2854-2860.	2.1	12

#	Article	IF	CITATIONS
37	Synthesis, structural characterization, antibacterial activity, DNA binding and computational studies of bis(2-methyl-1H-imidazole κN3)silver(I)dichromate(VI). Journal of Molecular Structure, 2017, 1133, 591-606.	3.6	12
38	Theoretical insight into the impact of sumanene functionalization with BH and NH groups on its ozone addition features. Vacuum, 2017, 136, 82-90.	3.5	11
39	Hetero-fullerenes C59M (M = B, Al, Ga, Ge, N, P, As) for sulfur dioxide gas sensing: Computational approach. Chemical Physics, 2020, 530, 110606.	1.9	11
40	Relative electrophilicity and aromaticity. Chemical Physics Letters, 2010, 484, 363-367.	2.6	10
41	Tailoring C24S12 and C16S8 sulflowers with lithium atom for the remarkable first hyperpolarizability. Chemical Physics Letters, 2018, 709, 33-40.	2.6	10
42	A theoretical study on pristine and doped germanium carbide nanoclusters. Journal of Materials Science: Materials in Electronics, 2014, 25, 4193-4199.	2.2	9
43	Theoretical investigations of interactions between boron nitride nanotubes and drugs. , 2016, , 59-77.		9
44	In silico investigation of the ozone (O3) binding behavior to the B36 bowl-shaped structure. Adsorption, 2017, 23, 879-886.	3.0	9
45	Quantum chemical description of formaldehyde (HCHO), acetaldehyde (CH3CHO) and propanal (CH3CH2CHO) pollutants adsorption behaviors onto the bowl-shaped B36 nanosheet. Adsorption, 2017, 23, 1041-1053.	3.0	9
46	Tuning the electronicâ€optical properties of porphyrinâ€like porous C ₂₄ N ₂₄ fullerene with (Li ₃ O) _{nÂ=Â(1–5)} decoration. A computational study. Applied Organometallic Chemistry, 2019, 33, e4654.	3.5	9
47	Sensing of ozone (O3) molecule via pristine singe-walled aluminum nitride nanotube: A DFT study. Superlattices and Microstructures, 2016, 89, 390-397.	3.1	8
48	Computational evaluation of the remarkable electro-optical responses of the multilithiated pristine and heterosubstituted sumanenes. Chemical Physics Letters, 2017, 678, 51-58.	2.6	8
49	Endohedral M@B 40 (M = Na and Ca) metalloborospherenes as innovative potential carriers for chemotherapy melphalan drug: A theoretical study. Applied Organometallic Chemistry, 0, , e6411.	3.5	8
50	Electronic and nonlinear optical characteristics of the LiB n (n = 4–11) nanoclusters: A theoretical study. Microelectronic Engineering, 2017, 183-184, 64-68.	2.4	7
51	Functionalized olympicene (C19H12) as anode material for Li-ion batteries: a DFT approach. Monatshefte Für Chemie, 2019, 150, 1745-1751.	1.8	6
52	Exploring enthalpies of formation of imidazolium-, pyridinium-, and pyrrolidinium-based ionic liquids with dicyanamide anion using quantum chemical methods. Journal of Molecular Liquids, 2020, 308, 113137.	4.9	6
53	The impact of intramolecular H-bonding on the aromatic character of substituted penta-fulvenes. Computational and Theoretical Chemistry, 2013, 1017, 31-36.	2.5	5
54	Carbon monoxide monitoring using pristine and Cu-functionalized aluminum nitride and silicon carbide nanotubes; DFT study. Journal of Molecular Liquids, 2015, 204, 147-155.	4.9	5

#	Article	IF	CITATIONS
55	Probing the adsorption behavior of oxazole and isoxazole heterocyclic compounds onto B ₁₂ N ₁₂ nanocluster surface in gas and aqueous mediums through DFT calculations. Applied Organometallic Chemistry, 2018, 32, e4543.	3.5	5
56	A computational study on the electro-optical characteristics of C 2n (BN) 12-n (n = 1–11) hetero-nanoclusters: Toward the remarkable features by the encapsulation via alkali metals. Journal of Molecular Liquids, 2017, 233, 236-242.	4.9	4
57	Exploring the electroâ€optical properties of conjugated polymers based on oligoâ€selenophene and oligo(3,4â€ethylenedioxyselenophene). Applied Organometallic Chemistry, 2019, 33, e4962.	3.5	4
58	Silicon carbide nanotubes (SiCNTs) serving for catalytic decomposition of toxic diazomethane (DAZM) gas: a DFT study. Molecular Physics, 2018, 116, 414-422.	1.7	3
59	The teetotum cluster Li ₂ FeB ₁₄ and its possible use for constructing boron nanowires. Physical Chemistry Chemical Physics, 2020, 22, 15013-15021.	2.8	3
60	A study on the influence of intramolecular O Hâ <x (x="O" <mml:math="" altimg="si1.gif" and="" aromaticity="" bond="" by="" derivatives,="" formation="" heptafulvene="" hydrogen="" in="" is="" methylene="" of="" on="" overflow="scroll" replaced="" s)="" the="" which="" xmlns:mml="http://www.w3.org/1998/Math/MathML"><mml:mrow><mml:msubsup><mml:mrow><mml:mtext>AlH</mml:mtext></mml:mrow><mml:mrow><mml:mrow><mml:mtext>AlH</mml:mtext>2014, 1039, 21-27.</mml:mrow></mml:mrow></mml:msubsup></mml:mrow></x>	2.5 Il:mrow><	2 mml:mn>2
61	Evaluation of the Electrophilicites and Band Gaps of Conductive Polymers: A New Model. Macromolecular Theory and Simulations, 2012, 21, 529-534.	1.4	Ο